The Role of Ventilation
15th AIVC Conference, Buxton, Great Britain
27-30 September 1994

Natural Ventilation Through a Single Opening - The Effects of Headwind

G M J Davies, M J Holmes

Arup Research & Development, Ove Arup & Ptners, 13 Fitzroy Street, London W1P 6BQ

SYNOPSIS

The airflow between a warm room and cool exterior can be significantly affected by an external headwind. Pollutant concentrations within the space depend on the relative sizes of the wind and the undisturbed stack driven flow. Two scenarios are described.

Firstly, a space is filled initially with buoyant polluted air. The space is then naturally ventilated through a single opening. In the "no wind" case, a gravity current of external air flows into the space. All the polluted air is expelled from the room. At high wind speeds the turbulence associated with the headwind produces mixing just inside the doorway. Under some conditions, ventilation levels are reduced. The second scenario considered is the natural ventilation of a space containing a continuous source of buoyant pollutant. For weak headwinds, fresh external air flows into the room and the pollutant concentration in that lower layer remains close to zero. High headwind speeds again generate doorway mixing. Air flowing into the space becomes contaminated with pollutant

These flows were studied experimentally using small-scale saline modelling techniques. Simple mathematical models are presented which agree closely with the experimental results. In both the transient and continuous cases, an increase in the headwind could lead to reduction in ventilation and an increase in internal pollutant levels. Natural ventilation through a single opening is not necessarily enhanced by wind.

LIST OF SYMBOLS

B	Buoyancy flux per unit width in room (m^3s^{-3})
c_1	Pollutant concentration in upper layer
c_2	Pollutant concentration in lower layer
D	Height of doorway (and room)
e	Entrainment constant for continuous flows
E	Entrainment constant for transient flows at high Fr
Fr	Froude number
g	Gravitational acceleration
g'	Reduced gravitational acceleration
k	Constant of proportionality in equation for velocity of gravity current
K	Scaled volume flux per unit width through doorway
Pé	Péclet number
Q	Volume flux per unit width down the room at high Fr
Q_1	Volume flux per unit width carried by gravity current
Q_e	Volume flux per unit width entrained into buoyant plume
Q_s	Source volume flux per unit width
Q_0	Volume flux per unit width across the doorway at high Fr
Q_{gc}	Volume flux carried by theoretical half-height gravity current
Re	Reynolds number
u_1	Gravity current velocity

u_{gc}	Gravity current velocity at $Fr = 0$
U	Headwind speed
$\delta\rho$	Density difference between interior and mixed region in high Fr model
$\Delta\rho$	Density difference between interior and exterior
ϕ	Scaled density difference
κ	Diffusivity
λ	Fractional height of room occupied by gravity current
ν	Kinematic viscosity
ρ	Ambient density
σ	Scaled volume flux per unit width down the room

1. Introduction

Natural ventilation is increasingly been seen as a viable option to air-conditioning for the removal of internally generated pollutants and heat. It is generally assumed that satisfactory ventilation air flows will be achieved by means of cross ventilation driven by the combination wind and buoyancy forces. One central feature of such designs is that the client is encouraged to avoid closed perimeter offices [1]. There are however many circumstances when cellular offices are desirable, privacy and status for example. In general such office spaces will be relatively shallow and experience suggests that there is little need to worry about internal environmental conditions with single sided ventilation.

There is however always the desire to stretch things to the limit so the question of how deep can a space be before it is essential to use cross ventilation arises. One experimental study [2] suggests that acceptable ventilation can be achieved within a 10m space. Internal gains in that case were not typical of modern commercial office spaces and further it is difficult to generalise the results of a single experiment. In particular it is difficult to isolate the relative effects of the two driving forces, wind and buoyancy. This paper presents an experimental and theoretical investigation with particular emphasis on the interaction of these two driving forces.

Airflows caused by temperature differences either side of an opening have been studied extensively in recent years. Early experimental work on stack driven flows is described in [3 - 6]. The incoming air flows through the doorway takes the form of a gravity current flowing into the room. The dynamics of gravity currents are well known and are described in [7].

A number of factors may influence such stack driven flows. One of the most significant of these is external wind. Air speeds through a typical doorway due to a temperature difference of 5°C are around $0.4 ms^{-1}$. Wind speeds are often of this magnitude or greater. Therefore, it might be expected that the effects of wind on buoyancy driven flow are considerable.

The different flows caused by different headwinds can be categorized in terms of an external Froude number. This Froude number is the ratio of external headwind velocity to a typical velocity produced by buoyancy alone. In the transient and continuous cases the Froude number is defined by

$$Fr = \frac{U}{\left(g\frac{\Delta\rho}{\rho}D\right)^{\frac{1}{2}}}, \quad \text{and} \quad Fr = \frac{U}{2\left(\frac{B}{2}\right)^{\frac{1}{3}}} \qquad (1)$$

respectively, where U is the headwind speed, B is the buoyancy flux per unit width, g is gravitational acceleration, $\Delta\rho/\rho$ is the fractional density difference and D is the height of the room. Note that zero headwind has $Fr = 0$. Buoyancy effects become negligible in the limit $Fr \rightarrow \infty$.

All experimental work was done using the saline modelling technique, the paper first presents the basis of that method and then details of the experiments followed by the development of a simple mathematical model.

2. Experimental Study

2.1 Modelling Techniques

2.1.1 Dynamical Similarity

Water was used as the working fluid for the experiments. Density differences (corresponding to temperature differences) were produced by adding of brine. The validity of representing full-scale airflows by small-scale water flows requires that the ratios of the important forcing terms in the equations of motion are the same at small-scale as at full-scale. This dynamical similarity is equivalent to matching the important dimensionless parameters of the flows. For buoyancy driven airflows the important dimensionless numbers are the Reynolds number, Re, and the Péclet number, $Pé$. These are defined by

$$Re = \frac{UD}{\upsilon} \quad \text{and} \quad Pé = \frac{UD}{\kappa}. \qquad (2)$$

For ventilation airflows, the Reynolds and Péclet numbers are both high and the flows are turbulent. At such high values, it would be expected that the dependence of the flows on the values of Re and $Pé$ is not great.

2.1.2 Experimental Techniques

The experiments were carried out using a clear perspex room with rectangular cross-section. This modelled a section of a deep office with depth to height aspect ratio equal to five. A removable cover was placed on the upwind end of the room. For the transient experiments, the room was filled initially with dyed buoyant fluid. For all of the experiments, brine was the source fluid and was therefore more dense than the ambient environment. By viewing the experiment upside-down, the effect of buoyant fluid rising was achieved. This inversion was valid since density differences were small. The experiment was started by uncovering the end of the room. The flow modelled was that of single-sided ventilation of a deep office. This geometry was chosen for simplicity, with the flows in the interior being close to two-dimensional.

For the continuous experiments, a constant supply of dyed buoyant fluid was pumped into the space next to the closed end. The buoyant fluid was supplied through a line source occupying the full width of the room. The source was placed at the top of the room pointing downwards so that a downward flowing two-dimensional plume of dense fluid was produced. At full-scale, the source of buoyancy may be due to a heat source and no volume flux would be supplied to the room. For these experiments the volume flux was kept as low as possible (typically ten times less than the flux carried towards and away from the source).

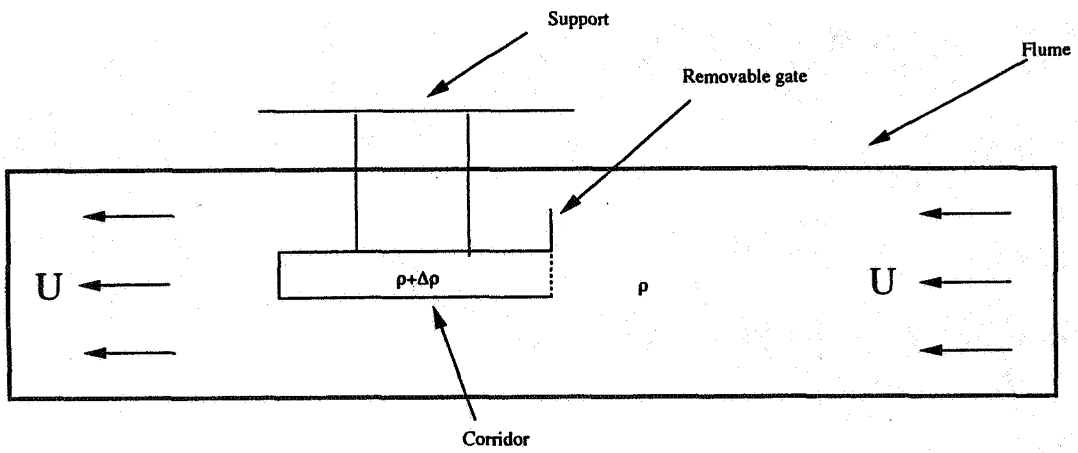

Figure 1. Experimental apparatus

To simulate an external headwind, the room was suspended in a much larger flume tank. The flume produced a time-independent uniform flow along its length and modelled an oncoming headwind. The experimental apparatus was as shown in figure 1. Video recordings were made of the experiments to enable measurements of velocities and other flow properties. Thermal exchanges with the walls of the room were neglected. This is a reasonable assumption provided that heat flux from the boundaries was much less than the heat flux associated with any buoyancy driven flow.

2.1.3. Experimental Parameter Ranges

The transient emptying of buoyant fluid from the room was studied for Froude numbers ranging from 0 to 11.4. The case $Fr = \infty$ was also investigated. For these experiments, the values of Reynolds number and Péclet number were approximately 5000 and 10^6 respectively. For the experiments with a steady source of buoyancy, Froude numbers lay between 0 and

7.7. Values of Reynolds number and Péclet number were similar to those for the transient experiments.

2.2 Transient Flows

2.2.1 Qualitative results

For flows driven by buoyancy only (*i.e.* $Fr = 0$) the observed flow was a gravity current occupying close to half the height of the room as shown in figure 2. The interface between inflow and outflow was situated approximately halfway up the room. The gravity current travelled at constant speed along the room and was reflected at the end. When the reflected gravity current had returned to the doorway, the interface ceased to be at half-height and the flow through the doorway was no longer quasi-steady.

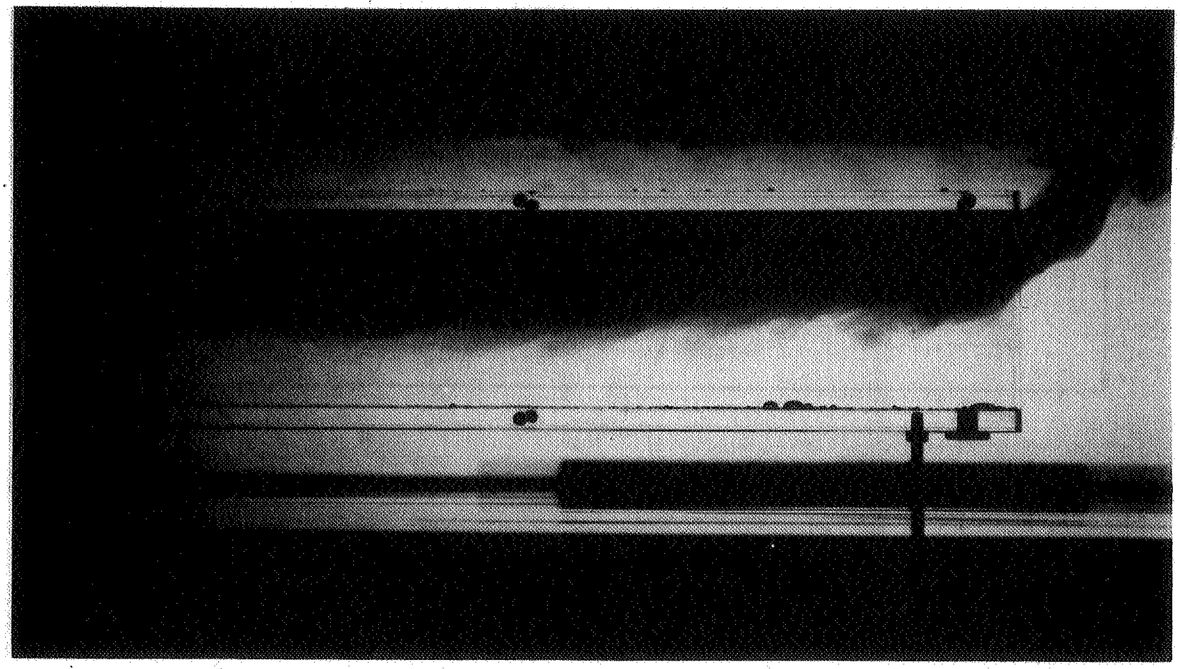

Figure 2. Gravity current at $Fr = 0$

For larger values of Froude number the interface between incoming and outgoing fluid was raised at the doorway as shown in figure 3. The different pressure distribution at the doorway due to the headwind affected the interface height. Within the room, the interface adjusted by sloping downwards and a gravity current flowed into the interior. At low Froude number, little mixing occurred between the two layers. Interfacial mixing near the doorway increased with Froude number. This increase appeared to be due to an increase in shear between the counterflowing layers.

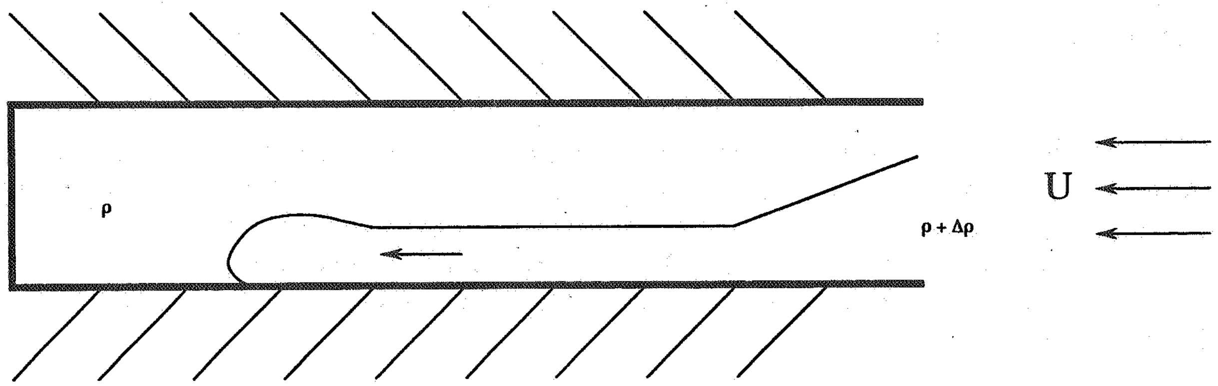

Figure 3. Raised doorway interface at intermediate *Fr*

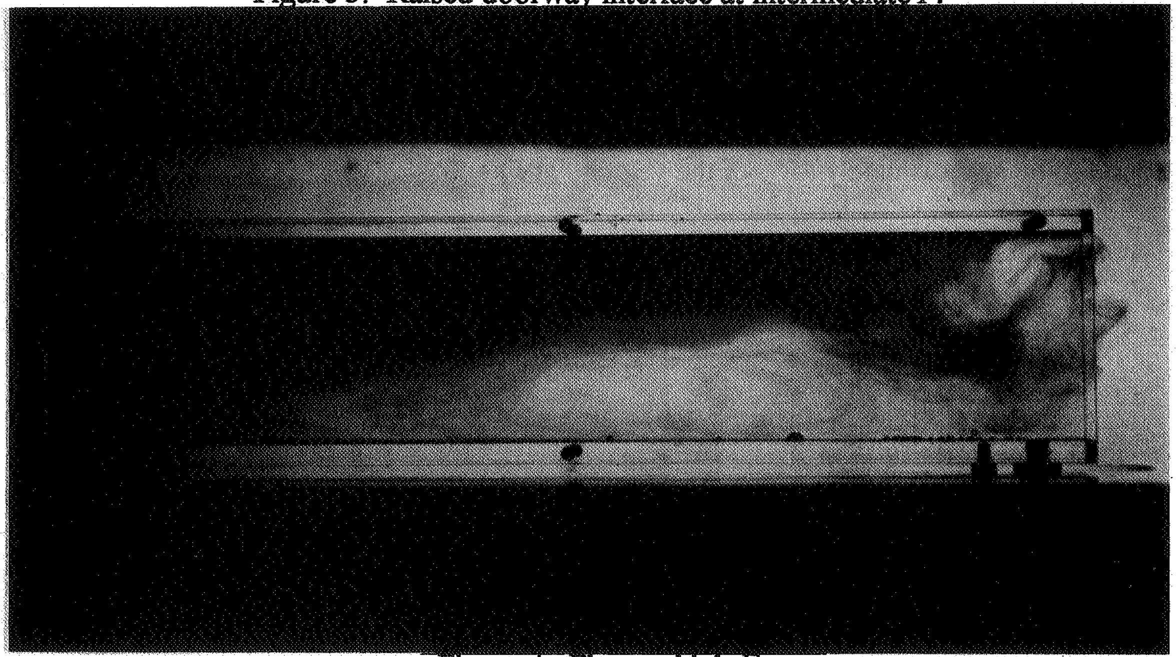

Figure 4. Flow at high *Fr*

For Froude numbers greater than $Fr \approx 8$, interfacial mixing had increased to the point where no clear interface existed between inflow and outflow at the doorway. For Froude numbers of this magnitude and higher, fluid within the room was observed to be well mixed near the doorway. Wind effects dominated the flow here. In spite of this, a gravity current was seen to flow from the mixed doorway region towards the interior as shown in figure 4. As a result of mixing, the gravity current contained both buoyant and ambient external fluid. The density difference driving the gravity current was less than that in the low Froude number cases. Therefore it was expected that the gravity current velocity would be lower than at $Fr = 0$.

At high Froude numbers, the flow between the doorway and the exterior was seen to be unsteady and irregular. Puffs of fluid of various sizes were seen leaving at random heights through the doorway.

In the case $Fr = \infty$, exterior fluid entered the room by means of a wind driven turbulent mixing process. Fluid was mixed across the doorway at a rate proportional to the wind speed. The amount of wind driven mixing reduced further down the room because turbulence was damped by viscosity. It is worth noting that the flow would be very different if the leeward end of the room were uncovered. In that case, a "plug" flow would rapidly purge the buoyant fluid from the room.

2.2.2 Quantitative results

The scaled velocities and scaled volume fluxes of the observed gravity currents are plotted against Froude number in figures 5 and 6. Note that the effect of interfacial mixing at high Froude number is to reduce both the velocity and volume flux associated with the gravity currents. Fractional heights occupied by gravity currents ranged from close to 0.5 at $Fr = 0$ to approximately 0.35 at $Fr = 11.4$. The velocity of the gravity current at high Froude number was found to be approximately 40% of the velocity at $Fr = 0$.

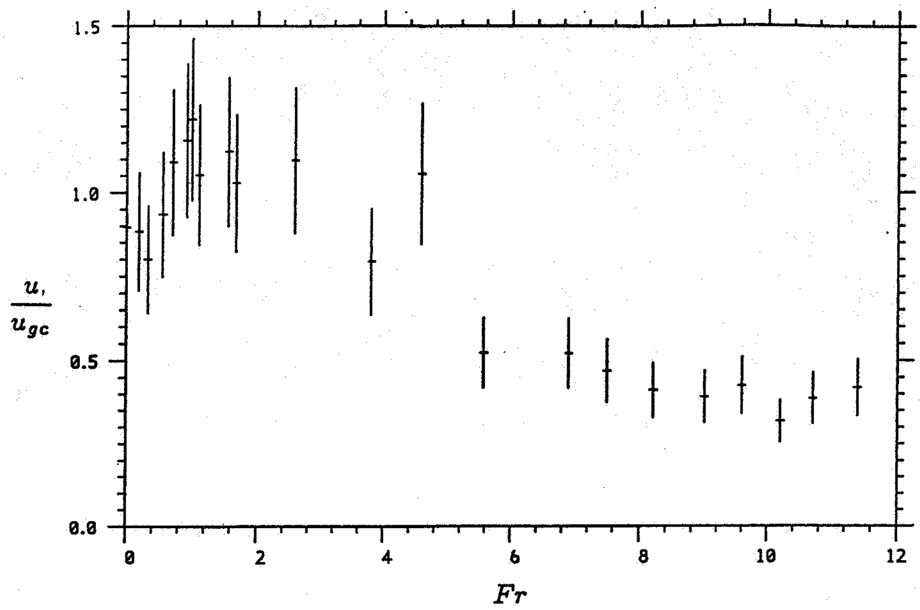

Figure 5. Scaled velocity plotted against *Fr*

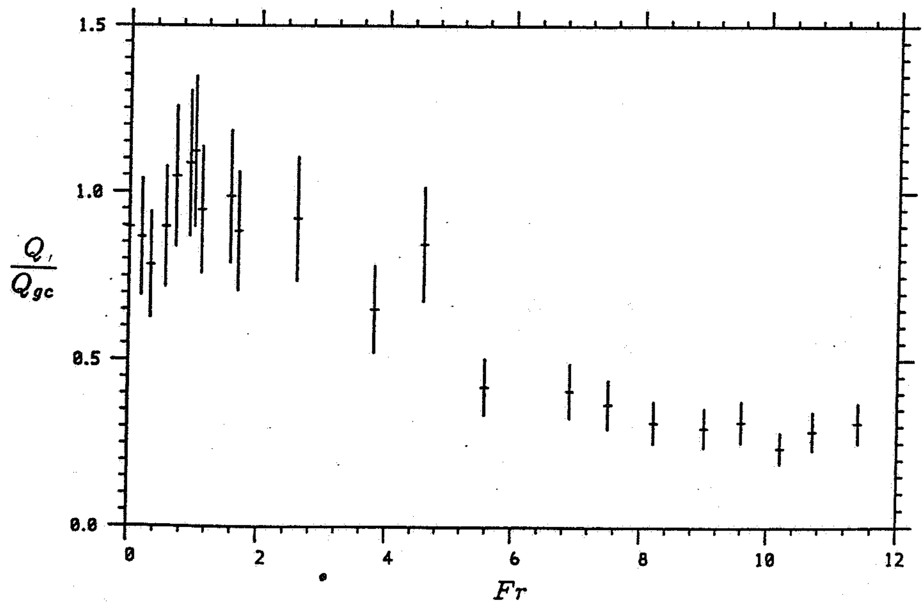

Figure 6. Scaled volume flux plotted against *Fr*

2.3 Continuous Flows

2.3.1 Qualitative results

The nature of the flow at $Fr = 0$ depended significantly on the source volume flux, Q_s. Varying the reduced gravity, $g' = g\Delta\rho/\rho$, did not noticeably affect the qualitative nature of the flow. For small values of Q_s, the buoyant plume entrained less fluid from the room than plumes produced by higher source volume fluxes. For this reason, low values of Q_s led to shallow gravity currents. After the gravity current head had left the room, the flow reached a steady state and a stable two-layer stratified flow was established within the room.

For intermediate Froude numbers ($1 \leq Fr \leq 4$), the only qualitative difference to the flow occurred near the doorway. Once again, the different pressure distribution caused by the headwind led to a shallowing of the outflow through the doorway. The influence of the wind, however, was localised to the region near the doorway. Further down the room, the flow was qualitatively similar to that at $Fr = 0$.

Further increases in Froude number again led to increases in interfacial mixing. For Froude numbers greater than $Fr \approx 7$ no interface between inflow and outflow at the doorway was apparent. The flow just within the doorway was dominated by the wind turbulence. Nonetheless, buoyancy dominated the flow within the room. The buoyant source plume appeared relatively unaffected by the external wind.

2.3.2 Quantitative results

Experimental measurements in the case $Fr = 0$ give the least squares fit relationship between u, the velocity in the buoyant layer, and B, the buoyancy flux per unit width of the source, as

$$u = (0.83 \pm 0.07)\, B^{(0.35 \pm 0.04)}, \qquad (3)$$

where $B = g'Q_s$. This value is close to the theoretical prediction for layers each occupying half the height of the room $u = (B/2)^{1/3}$.

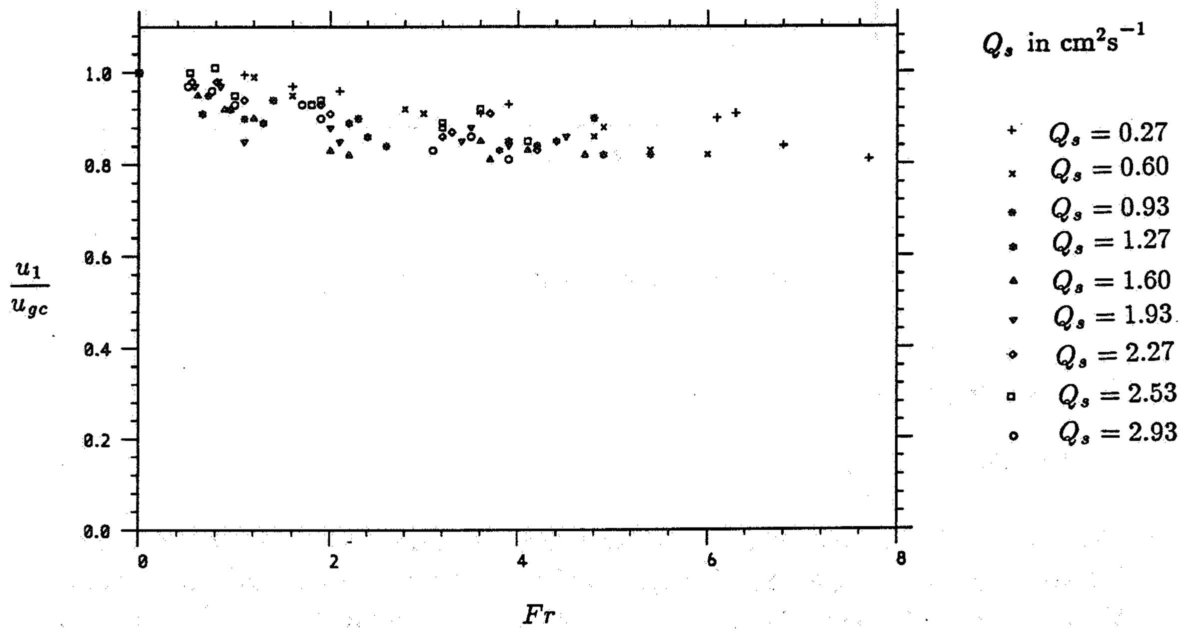

Figure 7. Scaled velocity of buoyant layer plotted against Fr

Figure 7 shows a plot of scaled velocity within the buoyant layer against Froude number. The velocities are scaled with experimentally measured values at $Fr = 0$.

Unlike the transient case of §2.2, velocities within the buoyant layer decrease only slightly with increasing Froude number. This result demonstrates that the entraining plume at the closed end of the room strongly influences the two-layer exchange flow. The observation also suggests that the amount of entrainment into the plume is not drastically affected by the density of fluid it entrains.

3. Mathematical Models

3.1 Transient Flows

3.1.1. Gravity Current Model at $Fr = 0$.

Inviscid dissipationless theory is used in [7] to predict that a gravity current flowing into an infinitely deep office would occupy half the height of the room and have a steady velocity

$$u = \frac{1}{2}(g'D)^{\frac{1}{2}}, \tag{4}$$

where $g' = g\Delta\rho/\rho$ is the reduced gravity. In reality, energy loss occurs. Experimental measurements described in [8] found considerable variations in velocity with changing height. They expressed the gravity current velocity as

$$u = k(\lambda)(g'D)^{\frac{1}{2}}, \tag{5}$$

where λ is the fractional height of the gravity current. The results of [8] found values including $k(0.3)=0.41$ and $k(0.05)=0.3$. The experiments at high *Fr* revealed a gravity current with $\lambda=0.35$ corresponding to $k=0.43$.

3.1.2 Mixed Doorway Region Model At High Froude Number

Consider a flow régime illustrated in figure 8. Assuming the flow to be steady, it can be deduced that

$$(\rho + \Delta\rho)Q_0 - (\rho + \delta\rho)Q_0 + \rho Q - (\rho + \delta\rho)Q = 0. \tag{6}$$

It is then possible to solve this equation to produce an equation relating the volume flux carried from the mixed region to the interior and the volume flux entrained through the doorway.

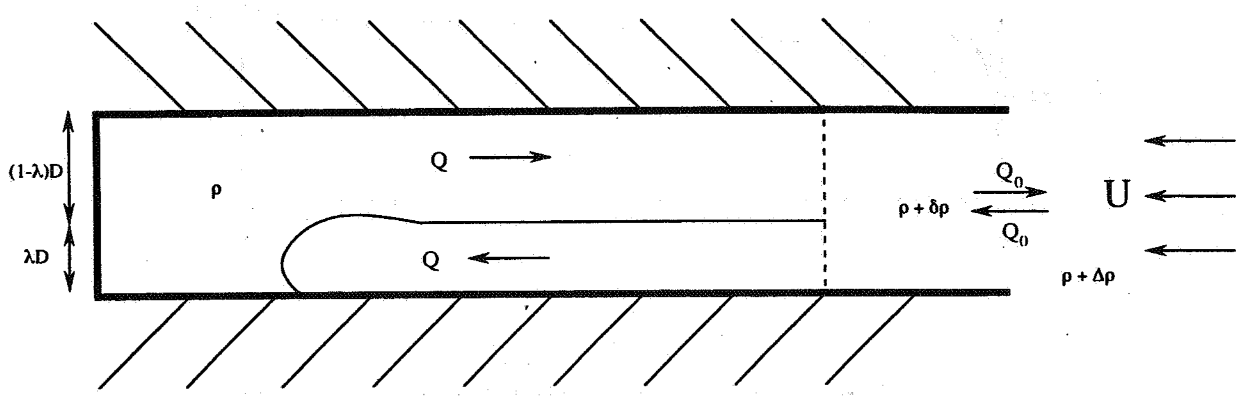

Figure 8. Model of flow at high *Fr*

The volume flux per unit width carried into the interior, Q, is given by

$$Q = 4k\lambda\, \phi^{\frac{1}{2}} Q_{gc} \tag{7}$$

where

$$Q_{gc} = \frac{D}{4}\left(g\frac{\Delta\rho}{\rho}D\right)^{\frac{1}{2}} . \tag{8}$$

Equations (7) and (8) together imply

$$(\sigma + K)\sigma^2 - 16k^2\lambda^2 K = 0 \tag{9}$$

where $\sigma = Q/Q_{gc}$ and $K = Q_0/Q_{gc}$. Using an entrainment assumption in the spirit of that proposed in [9], it is possible to hypothesize a value for the volume flux across the doorway. Assuming that the mixing effects of the wind turbulence drive the flow across the doorway then the volume flux across the doorway can be estimated as

$$Q_0 = \frac{DEU}{2}, \tag{10}$$

where E is an entrainment constant.

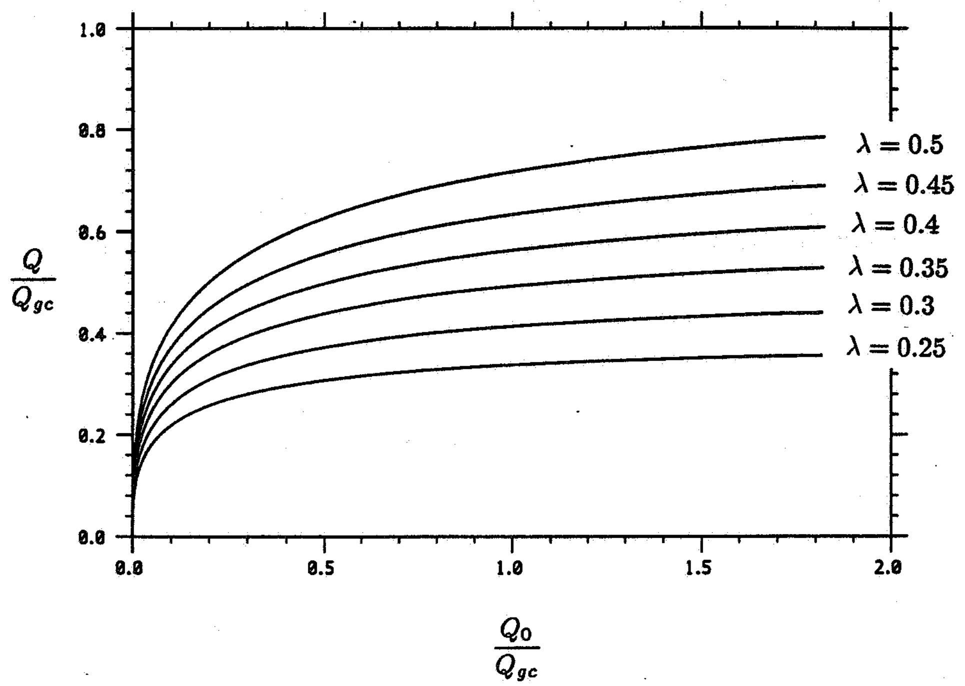

Figure 9. Flux along the room plotted against flux through the doorway

Figure 9 shows a plot of flux along the room as a function of flux through the doorway. The results are shown for a range of values of λ. Corresponding values of k are taken from [8]. The experimental results suggest a value $E = 0.003$ as the appropriate entrainment constant. This value of entrainment constant is considerably lower than that for a plume or jet.

3.2 Continuous Flows

3.2.1 The Entrainment Counterflow at $Fr = 0$

One way to analyse the flow at $Fr = 0$ is to consider the amount of entrainment into the buoyant source plume at the closed end of the room. Using an entrainment assumption it is possible to predict the volume flux of fluid entrained into the plume. Then, the total volume flux carried in the buoyant layer is simply

$$Q = Q_e + Q_s \tag{11}$$

For a two-dimensional buoyant plume (see [10]), plume theory predicts that the mean velocity within the plume is given by

$$u = \left(\frac{B}{e}\right)^{\frac{1}{3}} \tag{12}$$

where e is an entrainment constant. If λ is the fractional height occupied by the buoyant layer then the volume flux of fluid entrained can be predicted to be

$$Q_e = (1-\lambda) D e^{\frac{2}{3}} B^{\frac{1}{3}} \tag{13}$$

Conservation of mass then implies that

$$(Q_e + Q_s)^{\frac{3}{2}} = k\lambda\, D^{\frac{3}{2}} \left(g\frac{\Delta\rho}{\rho}\right)^{\frac{1}{2}} Q_s^{\frac{1}{2}} . \tag{14}$$

The experimental results lead to a value $e \approx 0.09$. This value is typical for buoyant plumes.

3.2.2 Mixed Doorway Region Model At High Froude Number

For this continuous case, a simple model can be constructed for the flow at high Froude number. The model is similar to that in the transient case. This model predicts that the velocity of the buoyant layer at high Froude number will be less than that at $Fr = 0$ by a factor

$$\left(\frac{Q_0}{Q_0 + Q_s}\right)^{\frac{1}{3}} \tag{15}$$

Close agreement is found between experimental data and the model. Using an entrainment hypothesis similar to that described for the transient case described above, it is possible to estimate the entrainment into the doorway region. Comparison with the experiments suggests a value $E = 0.008$. This value is higher than that predicted for the transient case. This result could suggest that there are fundamental differences between the mixed doorway regions in the transient and continuous cases.

3.2.3 Pollutant Dispersion

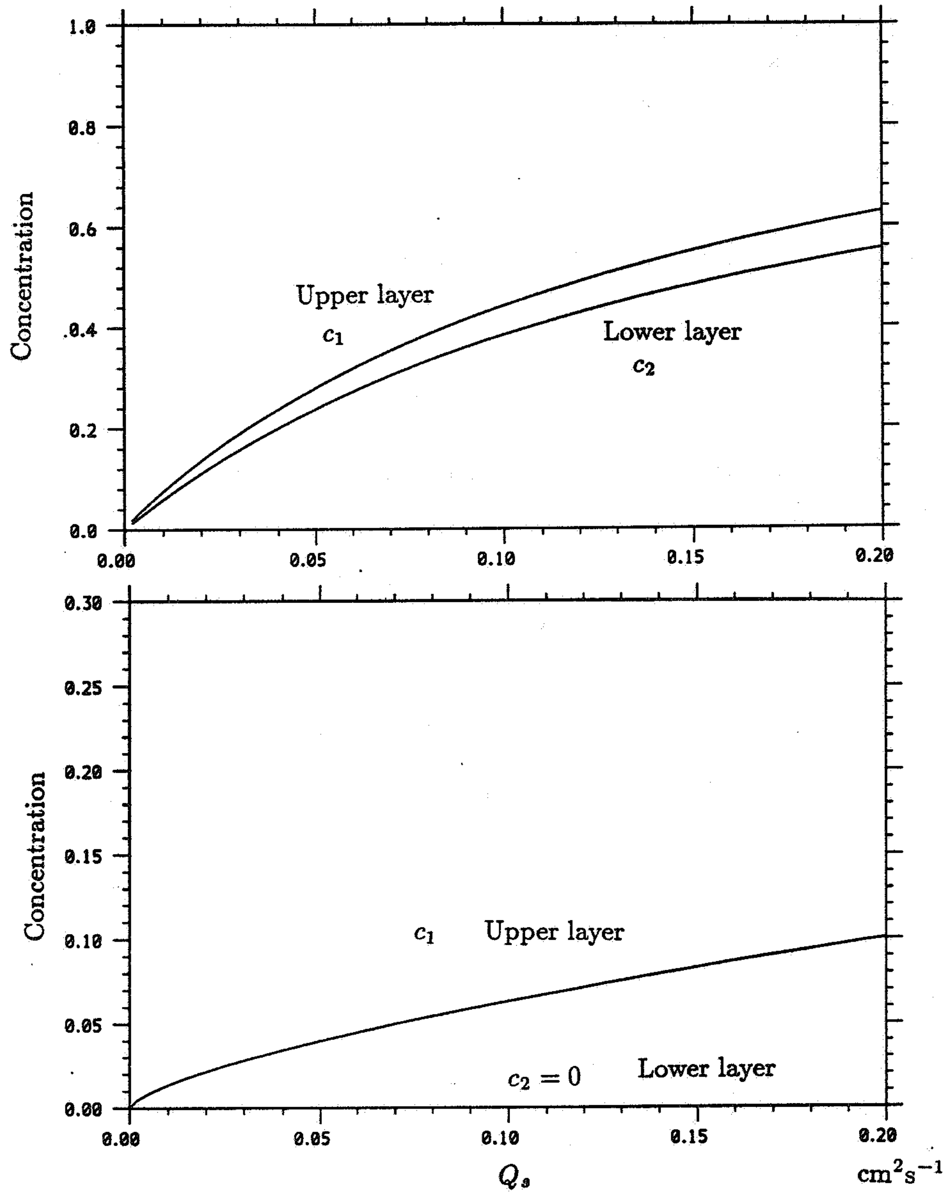

Figure 10. Concentration predictions at high and low *Fr*

The continuous source of buoyancy described above could well be a leaking gas pipe. In this case, the concentrations of gas in both the upper and lower layers within the room are of some significance. Mixtures of natural gas and air with 5 to 15% gas are potentially explosive. When wind effects are small, the concentration of gas within the lower layer is close to zero. This would not be the case in very windy external conditions where mixing at the doorway leads to some natural gas being carried from the doorway region back down the room. Using the model described in the previous section it is possible to predict gas concentrations within both the upper and lower layers. These concentration predictions are shown in figure 10 as functions of source volume flux both at high and low values of Froude number. The predictions assume $E = 0.008$ as suggested by the continuous experiments.

4. Conclusions

Several conclusions can be drawn from these studies. Firstly, an increase in headwind can be detrimental to single-sided natural ventilation. Air change rates can be reduced. Polluted air from the buoyant layer can be mixed into the lower layer, increasing levels of pollutant there. The second main deduction is that, for single-sided ventilation, wind effects are largely confined to the region near the doorway. Buoyancy forces dominate the flows away from the doorway region.

The results in this study are consistent with full scale tests carried out on a test room [2] and on a test house [11]. Buoyancy driven flows through a single opening under the additional influence of turbulent mixing on one side of the opening were studied in [12]. He also observed a decrease in volume flux through the doorway

Acknowledgements

This work was carried out while G.M.J.D. was studying for a Ph.D. degree at the Department of Applied Mathematics and Theoretical Physics, University of Cambridge under the supervision of Dr. P.F. Linden. The Ph.D. study was funded by a U.K. Science and Engineering Council CASE Award co-sponsored by the Ove Arup Partnership.

REFERENCES

[1] Holmes M, J. Design for ventilation. 6th AIC Conference, Het Meerdal Park, Netherlands, 1985.

[2] Van der Maas, J. (ed.). Heat loss and buoyancy and wind driven flow through an open window in one wall only. *Air flow through large openings in buildings. I.E.A./E.C.B. ANNEX 20 (Technical report)*, 1992.

[3] Brown, W.G. and Solvason, K.R. Natural convection through rectangular openings in partitions. *Int. J. Heat & Mass Transfer* **5**, 1962, pp859-868.

[4] Brown, W.G., Wilson, A.G. and Solvason, K.R. Heat and moisture flow through openings by convection. *J. Am. Soc. Heating, Vent. and Air Conditioning Eng.* **5**, 1963, pp49-54.

[5] Shaw, B.H. Heat and mass transfer by natural convection and combined natural convection and forced air flow through large rectangular openings in a vertical partition. *Inst. of Mech. Engineers Conference* **CS19**, 1971, pp31-39.

[6] Shaw, B.H. and Whyte, W. Air movement through doorways - the influence of temperature and its control by forced airflow. *J. Inst. Heating and Ventilation Eng.* **42**, 1974, pp210-218.

[7] Benjamin, T.B. Gravity currents and related phenomena. *J. Fluid Mech.* **31**, 1968, pp209-248

[8] Simpson, J.E. and Britter, R.E. The dynamics of a gravity current head. *J. Fluid Mech.*, **94**, 1979, pp477-495.

[9] Morton, B.R. Taylor, G.I. and Turner, J.S. Turbulent gravitational convection from maintained and instantaneous sources. *Proc. Roy. Soc. A* **234**, 1956, pp1-23.

[10] Chen, C.J. and Rodi, W. Vertical turbulent buoyant jets - A review of experimental data. 1980, Pergamon Press.

[11] Wilson, D.J. and Kiel D.E. Gravity driven counterflow through an open door in a sealed room. *Building and Environment* **25(4)**, 1990, pp379-388.

[12] Kiel, D.E. Buoyancy driven counterflow and interfacial mixing. Ph.D. Thesis, University of Cambridge, 1991.